Früh-Green, G.L., Orcutt, B.N., Green, S.L., Cotterill, C., and the Expedition 357 Scientists
Proceedings of the International Ocean Discovery Program Volume 357
publications.iodp.org

doi:10.14379/iodp.proc.357.106.2017

Northern sites[1]

G.L. Früh-Green, B.N. Orcutt, S.L. Green, C. Cotterill, S. Morgan, N. Akizawa, G. Bayrakci, J.-H. Behrmann, C. Boschi, W.J. Brazelton, M. Cannat, K.G. Dunkel, J. Escartin, M. Harris, E. Herrero-Bervera, K. Hesse, B.E. John, S.Q. Lang, M.D. Lilley, H.-Q. Liu, L.E. Mayhew, A.M. McCaig, B. Menez, Y. Morono, M. Quéméneur, S. Rouméjon, A. Sandaruwan Ratnayake, M.O. Schrenk, E.M. Schwarzenbach, K.I. Twing, D. Weis, S.A. Whattam, M. Williams, and R. Zhao[2]

Keywords: International Ocean Discovery Program, IODP, *RRS James Cook*, Expedition 357, Site M0070, Site M0074, seabed drills, RD2, MeBo, Atlantis Massif, Atlantis Fracture Zone, Mid-Atlantic Ridge, Lost City hydrothermal field, serpentinization, detachment faulting, oceanic core complex, hydrogen, methane, deep biosphere, carbon cycling, carbon sequestration, contamination tracer testing

Contents

Operations

During Expedition 357, cores were recovered from two sites in the northern area of Atlantis Massif: Sites M0070 and M0074 (Figure **F1**; Table **T1**). Newly acquired multibeam data, combined with preexisting data sets, were evaluated prior to each site to guide the drill teams regarding the anticipated seabed conditions and slope.

Site M0070

Cores were recovered from three holes at Site M0070 (proposed Site AM-07A), with an average site recovery of 44.53%. In addition, a conductivity, temperature, and depth (CTD) cast was conducted prior to coring operations to acquire baseline geochemical and microbiological information about the surrounding waters. The water depth was 1140.50 m with no tidal range. The total time spent on station was 2.46 days.

Hole M0070A

The vessel was on station at Site M0070 at 1212 h on 8 November 2015 and settled into dynamic positioning (DP) mode following a short multibeam survey over the area. The CTD sensor package with Niskin bottles was deployed at 1212 h. At 1259 h, the CTD was 1.7 m off the bottom, and the first three Niskin bottles were fired. Two further Niskin bottles were fired on the way up, with a final one fired near the surface (see Table **T5** in the Expedition 357 summary chapter [Expedition Scientists, 2017c]). The CTD was recovered on deck at 1334 h on 8 November. The vessel position was adjusted so that the DP center was located over the stern deployment position for the Meeresboden-Bohrgerät 70 (MeBo) drill.

The MeBo was deployed at 1405 h, and by 1604 h the drill was on the seafloor after mid–water column systems checks. The rig was leveled to ensure the overshot was central over the breakout table, and at 1748 h coring operations commenced. At 2148 h and with 1.70 m of penetration, rotation of the drill rod stopped due to "sticky" conditions. The bottom-hole assembly (BHA) was recovered and a new BHA put down the hole, changing from a surface set to a G4 bit. At 2040 h, numerous bubbles were observed on the camera feed from the MeBo drill. The MeBo stopped coring, and the bubbles appeared to stop, accompanied by noticeable deviation in the water sensor package methane sensor readings (see **Sensor package data**). The MeBo started coring again at 2050 h, continuing until 0228 h on 9 November, when the overshot wire snapped while trying to recover core Run 3. The British Geological Survey RockDrill2 (RD2) was put on standby and made ready for deployment. The MeBo was recovered on deck by 0506 h, and an assessment was made of the repairs required (overshot wire and a transformer problem on the HV unit). The vessel departed the site at 1000 h on 9 November.

In summary, three coring attempts were made in Hole M0070A to a maximum depth of 4.00 m with 52.25% recovery.

Hole M0070B

After conducting a deep-water CTD cast over the Mid-Atlantic Ridge (MAR), the sea state calmed enough to deploy the RD2. The

[1] Früh-Green, G.L., Orcutt, B.N., Green, S.L., Cotterill, C., Morgan, S., Akizawa, N., Bayrakci, G., Behrmann, J.-H., Boschi, C., Brazelton, W.J., Cannat, M., Dunkel, K.G., Escartin, J., Harris, M., Herrero-Bervera, E., Hesse, K., John, B.E., Lang, S.Q., Lilley, M.D., Liu, H.-Q., Mayhew, L.E., McCaig, A.M., Menez, B., Morono, Y., Quéméneur, M., Rouméjon, S., Sandaruwan Ratnayake, A., Schrenk, M.O., Schwarzenbach, E.M., Twing, K.I., Weis, D., Whattam, S.A., Williams, M., and Zhao, R., 2017. Northern sites. *In* Früh-Green, G.L., Orcutt, B.N., Green, S.L., Cotterill, C., and the Expedition 357 Scientists, *Atlantis Massif Serpentinization and Life*. Proceedings of the International Ocean Discovery Program, 357: College Station, TX (International Ocean Discovery Program). http://dx.doi.org/10.14379/iodp.proc.357.106.2017

[2] **Expedition 357 Scientists' addresses.**

MS 357-106: Published 4 February 2017

Figure F1. Detailed site and hole location images for Sites (A) M0070 and (B) M0074 overlain onto DSL120 sonar imagery (from Blackman et al., 2002) in two different swath orientations and the newly acquired 50 m resolution multibeam bathymetry.

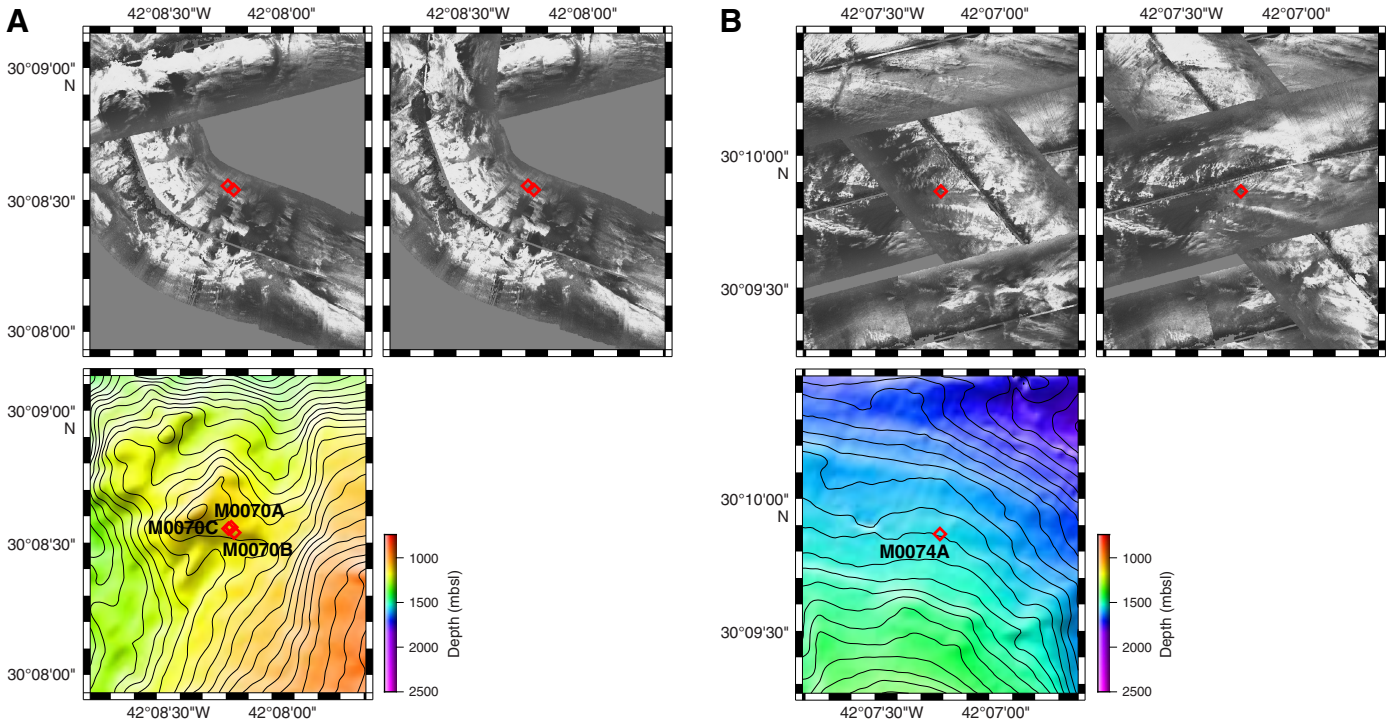

Table T1. Northern sites hole summary. **Download table in .csv format.**

Date coring operations commenced (2015)	Hole	Proposed site	Latitude	Longitude	Water depth (m)	Drill	Number of cores	Interval cored (m)	Core recovered (m)	Core recovery (%)	Interval open holed (m)	Penetration depth (mbsf)	Time on site (days)
8 Nov	M0070A	AM-07A	30°8.553N	42°8.188W	1140.50	MeBo	3	4.00	2.09	52.25	0.00	4.00	0.94
14 Nov	M0070B	AM-07A	30°8.538N	42°8.163W	1140.50	RD2	1	1.30	0.38	29.23	0.00	1.30	0.22
22 Nov	M0070C	AM-07A	30°8.544N	42°8.194W	1140.50	MeBo	3	5.21	2.21	42.42	0.00	5.21	1.30
30 Nov	M0074A	AM-09A	30°9.865N	42°7.315W	1550.00	MeBo	1	2.68	0.86	32.09	0.00	2.50	0.23

vessel transited to Site M0070, arriving and settling into DP mode by 1640 h on 14 November 2015. The vessel was in position at 1710 h, and the RD2 was deployed at 1747 h, landing on the seafloor at 1852 h. Coring started at 1910 h, but the BHA stalled at 1921 h. At 2039 h, all communications were lost with the RD2. The MeBo started predive checks in case the RD2 needed to be recovered. At 2053 h, after attempts to restart communications, the RD2 had to be recovered, initially with the BHA protruding from the bottom of the drill. At ≈467 m water depth at 2117 h, communications came back online, and the BHA could be retracted for a normal recovery. The RD2 was on deck and secure by 2150 h on 14 November. The vessel was given clearance to begin the transit to Site M0073 for a MeBo deployment.

In summary, one coring attempt was made in Hole M0070B to a maximum depth of 1.30 m with 29.23% recovery.

Hole M0070C

The vessel arrived on station at 0720 h on 22 November 2015 after stopping a multibeam survey of the eastern conjugate margin when weather conditions began to improve. Due to sea swell from three directions, it took time to find the best heading, and no operations were able to commence until 0818 h. At this time, the RD2 was launched for a wet test and was recovered on deck at 0900 h. Owing to marginal weather conditions for drill deployment, the vessel maintained position waiting on weather.

The sea state and swell slowly calmed, and at 1546 h the Master of the Vessel gave permission for operations to start with MeBo deployment. The MeBo was in the water at 1659 h and on the seafloor by 1835 h. Coring started at 1916 h. Penetration slowed at 1.17 m, and the decision was made to take out the BHA (surface-set bit) and replace with a new BHA (G4 bit) and second core barrel. This process was completed by 2056 h with the start of core Run 2. At 0230 h on 23 November, the MeBo penetrated 5.21 m with the third core barrel. However, there were problems in getting core Barrel 4 into the BHA, and after multiple attempts, it was decided to remove this BHA and replace it with the third one carried on the magazines. Because of broken magazine retainers, it was not possible to remove the third BHA from the magazine, so the second BHA was reinserted into the borehole in an attempt to ream back into the hole to log and install a borehole plug. Reentry proved difficult, and the onboard cameras indicated that the hole was blocked near the surface. After 1 m of reaming, the hole was aborted, and neither logging nor borehole plug deployment was attempted. On recovery, it was noted that the shoe, liner, and core had been left inside the second BHA

when the third core barrel was removed. This likely caused the initial problems with inserting Barrel 4. Additionally, although triggered, the Niskin bottles had failed to fire.

The MeBo was recovered on deck by 1511 h, and the vessel began to transit to Site M0068 for an RD2 deployment while the MeBo underwent repairs.

In summary, three coring attempts were made in Hole M0070C to a maximum depth of 5.21 m with 42.42% recovery.

Site M0074

Cores were recovered from one shallow hole at Site M0074 (proposed Site AM-09A), with 32.09% recovery. The water depth was 1550.00 m with no tidal range. The total time spent on station was 0.23 days.

Hole M0074A

At 0824 h on 13 November 2015, we temporarily halted the multibeam survey of the Atlantis Massif complex to conduct a CTD cast at Site M0074. This cast would obtain the baseline water information required for drilling the site at a later date and make the best use of the current "waiting on weather" status applicable to drilling operations. The CTD commenced at 0853 h, reaching approximately 1.3 m off the seafloor, and was back on deck and secure by 1042 h. Three Niskin bottles were fired near the seafloor, two were fired mid–water column, and one was fired near the surface (see Table **T5** in the Expedition 357 summary chapter [Expedition Scientists, 2017c]). Following this process, the multibeam survey of the Atlantis Massif complex recommenced.

The vessel returned to Site M0074 on 30 November at 1050 h. With the RD2 nonoperational and the MeBo limited to running only one core barrel length before having to return to deck (due to loss of tool handling capability in earlier operations), we planned to conduct a series of short holes with the MeBo to try to intersect the fault deformation zone. The MeBo was deployed at 1056 h and was on seafloor, after a mid–water column winch problem, by 1256 h. Coring commenced at 1305 h and rapidly progressed with 2.68 m penetration by 1325 h. Because no further tool handling operations could be attempted, coring terminated and the MeBo began recovery. Initial issues on recovery were followed by a mid–water column stop to replace a failed winch controller card at 1450 h. The MeBo was recovered on deck at 1535 h. With no further drill operations possible for either drill for the remainder of the expedition, it was decided to continue with the multibeam survey. The vessel departed the site at 1620 h on 30 November.

In summary, one coring attempt was made in Hole M0074A to a maximum depth of 2.68 m with 32.09% recovery. Because a metal split liner was used while coring Site M0074, the sediment core had to be transfered to a plastic liner and was highly disturbed in the process.

Lithology, alteration, and structure

Three holes were cored at Site M0070, located northwest of the Lost City hydrothermal field (Figure **F2**). Maximum core depth is 4.0 meters below seafloor (mbsf) in Hole M0070A with 2.09 m of core recovered, 1.3 mbsf in Hole M0070B with 0.38 m recovered, and 5.21 mbsf in Hole M0070C with 2.21 m of core recovered (Table **T1**). The lithology is similar in all three holes: sedimentary breccia in a carbonate matrix that includes foraminifers and predominantly contains clasts of unaltered basalt. Core 357-M0070B-1R contains fragments of serpentinized peridotite and metagabbro, Core 357-M0070C-2R contains serpentine sand, and Cores 357-M0070B-1R and 357-M0070C-1R contain fragments of metadolerite. The carbonate matrix in Cores 357-M0070A-2R and 357-M0070C-3R includes cavities that are partially filled by foraminiferal sand with subhorizontal laminations.

Figure F2. High-resolution multibeam bathymetry showing drilling locations. Contour interval = 20 m. A. Location of Holes M0070A–M0070C at the base of a ≈30 m high mound, likely a volcanic cone. B. Location of Hole M0074A on the striated detachment surface.

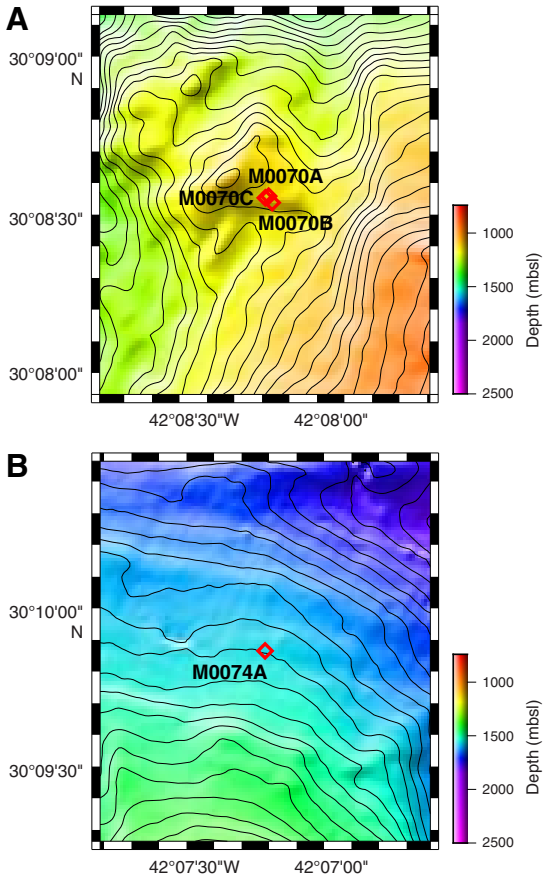

The basalt fragments in the breccia are mostly aphyric and vesicle poor. Vesicular fragments are found in Cores 357-M0070B-1R (with partial infill of the vesicles by clay minerals) and 357-M0070C-1R. Some basalt fragments in Cores 357-M0070A-2R and 327-M0070C-3R contain relict glass. Basalt fragments in Core 357-M0070C-2R have ≈1 cm thick gray alteration halos.

Hole M0074A is the northernmost site (Figure **F2**) and is very shallow (bottom of cored curated interval = 0.86 mbsf) (Table **T1**), consisting solely of unconsolidated fine foraminiferous sand.

More details can be found in the VCDs (see **Core descriptions**) and COREDESC in **Supplementary material**.

Rock types and igneous petrology

Three cores were recovered from Holes M0070A and M0070C, and only one core was recovered from Hole M0070B. They correspond to surficial sedimentary material, with basaltic and doleritic fragments contained within a variably cemented carbonate-matrix breccia. The clasts are dominated by aphanitic to microcrystalline basalts that are poorly to sparsely vesicular and variably altered. Oc-

casional plagioclase-phyric basalt fragments and minor metadolerite were observed.

Hole M0070A

Core 357-M0070A-1R consists of foraminiferous carbonate sand with small (up to 8 mm) basaltic fragments (Unit 1, 0–10 cm) and sedimentary basalt breccia (Unit 2). The basaltic breccia exhibits a poorly cemented matrix along the sides of angular basalt fragments. Basaltic clasts are poorly vesicular and in some cases plagioclase-phyric as defined by <1 mm, euhedral, and occasionally lath-like crystals. Larger fragments show alteration halos (Figure F3) and varying vesicularity between the core and rim.

Core 2R includes a relatively thin sequence of basalt breccia rubble (Unit 1, 0–21 cm) with loose, poorly vesicular (<1% vesicles) basalt clasts within the top 5 cm. This overlies a carbonate-cemented basaltic breccia (Unit 2), where some of the basalt clasts have remnant glassy margins.

Similar units were found in the following core (3R), which consists of sedimentary basaltic breccia with a carbonate matrix (Unit 1) overlying loose basalt clasts with light gray alteration halos (Unit 2). In general, basalt fragments are aphyric and poorly to sparsely vesicular (generally <1% vesicles); vesicles are rounded to subrounded.

Hole M0070B

Core 357-M0070B-1R consists of a sole unit of mixed fragments of mafic and lesser ultramafic rock fragments. Fragments of metagabbro and serpentinized peridotite are found in the uppermost interval (0–3 cm). The interval between 3 and 15 cm is composed of a single piece of altered vesicular basalt (10%–15% vesicles) with a microcrystalline matrix. The remaining interval (15–22 cm) is defined by a piece of vesicle-poor (<1% vesicles) basalt with a microcrystalline matrix.

Hole M0070C

Core 357-M0070C-1R contains a single unit of sedimentary basaltic breccia. Some basalt clasts are vesicular and exhibit alteration halos. The large fragment at 34–45 cm appears coarser grained and is likely metadolerite. This metadoleritic texture was also observed in thin section (1R-1, 35.5–37.5 cm). The remaining mafic fragments are aphyric basalt. The core catcher is the same sedimentary basalt breccia as the rest of Core 1R.

Core 2R contains fragments of sedimentary basaltic breccia. The consolidated sediment exhibits angular shards of oxidized basalt glass (<1 mm) and very small pale green fragments of what may be serpentine sand. Basalt clasts are aphyric and poorly vesicular (<1% vesicles). A piece of basalt glass if found between 42 and 47 cm.

Core 3R contains a sedimentary basaltic breccia overlying a consolidated basaltic breccia. The upper unit contains aphyric nonvesicular basalt fragments with carbonate sand linings along some of their margins. Relict glass is found in one basalt clast at 4–14 cm. The lower unit exhibits a consolidated carbonate infilling within the basaltic breccia. At 33–38 cm, layering is defined by alignment of small angular basalt shards. The core catcher also consists of a fractured moderately consolidated basaltic breccia.

Hole M0074A

Hole M0074A, the only hole drilled at this site, recovered a single 86 cm long unit of fossiliferous carbonate sand containing rare ≈5 mm lithic fragments of basalt.

Figure F3. Background alteration and alteration halos, Site M0070. A. Pale gray background alteration with dark gray and pale brown alteration halos (357-M0070A-1R-1, 14–23 cm). B. Dark gray background alteration with pale gray alteration halos (357-M0070C-2R-1, 17–26 cm).

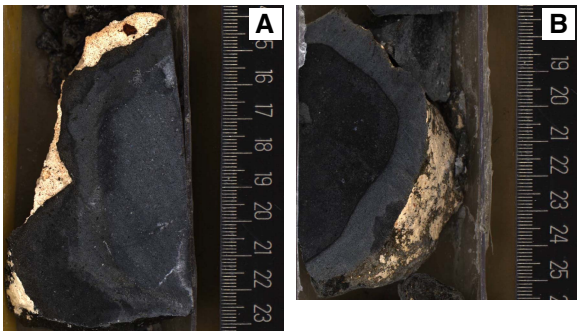

Figure F4. Vesicles lined by clay minerals (blue) and orange iron oxyhydroxides (357-M0070B-1R-1, 8–11 cm).

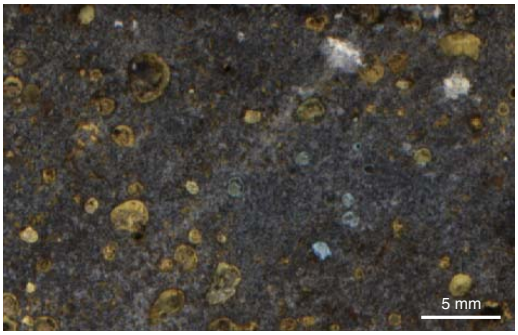

Alteration

Site M0070 is composed of basaltic breccia and basaltic rubble that underwent variable hydrothermal alteration that manifests as background alteration and alteration halos. Overall, the alteration intensity ranges from fresh to slight and is dominated by gray to orange alteration halos around the exterior edges of rubble pieces and clasts within the breccia (likely the result of low-temperature reaction with oxidized seawater).

Alteration of the cores recovered at Site M0070 has been classified as "other," which refers to hydrothermal alteration of the basaltic components in the breccia units. Background alteration is predominantly characterized by a uniform pale gray color. In thin section, minor replacement of clinopyroxene by clays was observed, but fresh plagioclase remains, supporting the observation of very minor hydrothermal alteration. Only one interval at Site M0070 exhibits different background alteration: throughout Core 357-M0070C-2R, the background alteration is dark gray. Alteration halos are either dark gray, pale gray, or pale brown, and the pale gray halos are restricted to Section 2R-1. The halos are between 5 and 35 mm in width and occur around the exterior edges of the pieces (Figure F3). Multiple chilled margins are present within the sedimentary breccia in Section 357-M0070A-2R-1, along with preservation of fresh glass fragments, further indicating minimal seawater interaction. In the most vesicular pieces (e.g., interval 357-M0070B-1R-1, 3–13 cm), thin coatings of pale blue saponite and orange iron oxyhydroxides were observed, but vesicles are generally not completely infilled (Figure F4).

Figure F5. Relative abundance of mineral phases identified by bulk powder XRD analysis, Site M0070. Colors correspond to mineral phases merged as groups (see **Core description** in the Expedition 357 methods chapter for mineral group definitions [Expedition 357 Scientists, 2017]). Numbers are semiquantitative abundances determined from fits to XRD peak patterns. Trace phases are subject to large uncertainties.

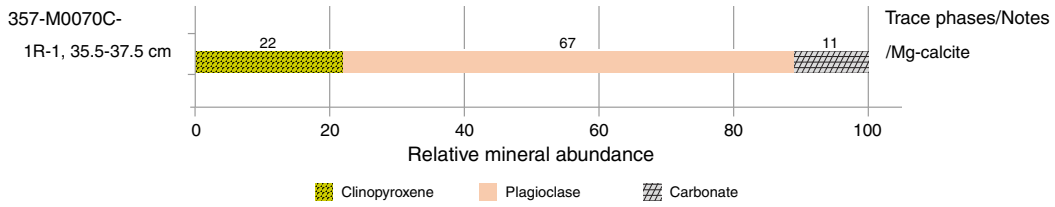

Table T2. X-ray diffraction results, Hole M0070C. Percentages were released by the software, sometimes with excess. Total sum <100% likely reflects the presence of amorphous or poorly crystallized material. Other poorly crystallized phases include MnFe oxides/hydroxides. **Download table in .csv format.**

Core, section, interval (cm)	All minerals present (proportion)
357-M0070C- 1R-1, 35.5–37.5	Clinopyroxene (22), plagioclase (67), carbonates (11)

Because Hole M0074A core material only consisted of sediment, alteration was not determined.

Veins, crosscutting, and overprinting relationships

Rare hairline (<0.1 mm) fractures are present in some Site M0070 pieces and are occasionally infilled with iron oxyhydroxides. Basaltic pieces and basaltic breccias record minimal hydrothermal alteration, and secondary minerals (clays and iron oxyhydroxides) are characteristic of low-temperature interaction with oxidized seawater. Such alteration is typical of basalts recovered from the ocean crust.

Overview of mineralogy from XRD data

Only a single sample was taken for X-ray diffraction (XRD) analysis from Site M0070 (Figure **F5**). The metadolerite sample mainly consists of primary phases: plagioclase (67%) and clinopyroxene (22%). Carbonate was also present (11%). XRD results for this site are provided in Table **T2**.

Structure

Site M0070 lies west of the western limit of the preserved striated detachment surface of Atlantis Massif at the foot of a ≈30 m high irregular mound (Figure **F2**). The three holes drilled the same structural unit composed of either loose or cemented clasts hosted in a carbonate matrix. A short interval of unconsolidated sandy sediment was recovered in Section 357-M0070A-1R-1. Clasts are solely basalts that contain vesicles and locally glass. Clasts vary in size from >10 cm to <1 mm (typically fine glass shards) within the lithified carbonate matrix.

Two types of matrix are observed: orange-brown and a later light tan deposit (Figure **F6**). The lighter colored matrix appears to fill voids and/or drape uncemented clasts and is younger than the glass-rich, orange-brown matrix deposit. The draping and infill geometry suggests that the core has not been rotated significantly since the emplacement of the lighter tan carbonate matrix.

The mound observed in bathymetry (Figure **F2A**) is likely a volcanic cone that has undergone faulting and/or mass wasting. Holes M0070A–M0070C, located at the base of this mound, likely drilled rubble on the flanks and at the base of this structure.

Figure F6. Sections of basalt breccia cemented by an early orange-brown matrix with voids infilled by later light tan carbonate. A. 357-M0070A-3R-1. B. 357-M0070C-1R-1.

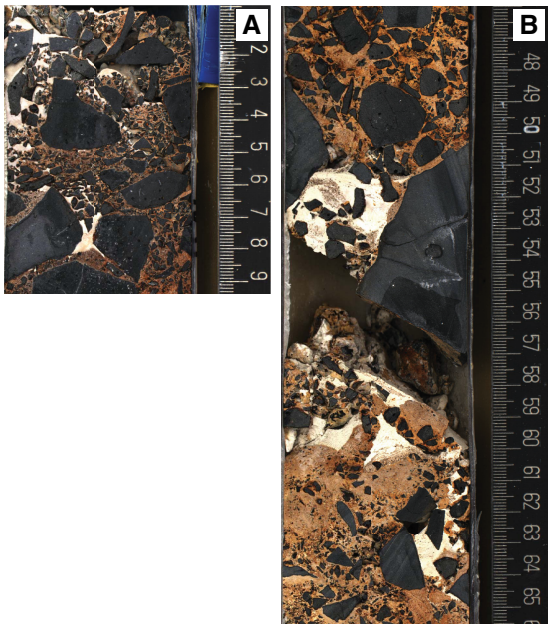

Site M0074 is the northernmost site, drilled over the detachment fault surface (Figure **F2B**). The detachment is corrugated parallel to the spreading direction; the site is located on the wall of one corrugation with an overall slope of ≈8°N. The site is situated at the summit of the detachment along an extension-parallel profile where the fault surface is subhorizontal in the east–west direction. At this location, only sediment was recovered, and no structures were measured.

Fluid chemistry

Inorganic and organic fluid chemistry

Cations and anions

As reported in detail in **Fluid chemistry** in the Eastern sites chapter (Expedition 357 Scientists, 2017a), salinities, major elements, trace elements, and anions measured in fluid samples during the expedition had concentrations comparable to bottom seawater (see Tables **T6**, **T7**, **T8**, and **T9** in the Eastern sites chapter [Expedition 357 Scientists, 2017a]). There was no detectable sulfide or ammonia (see Tables **T6** and **T10** in the Eastern sites chapter [Expedition 357 Scientists, 2017a]).

pH, alkalinity, and dissolved inorganic carbon stable carbon isotopic composition

As reported in detail in **Fluid chemistry** in the Eastern sites chapter (Expedition 357 Scientists, 2017a), the alkalinities and pH of fluid samples were similar to background seawater at all sites (see Table **T11** in the Eastern sites chapter [Expedition 357 Scientists, 2017a]), with the exception of pore water from carbonate sands from one of the central site locations (see Figure **F25** in the Eastern sites chapter [Expedition 357 Scientists, 2017a]).

Volatile chemistry

As reported in **Fluid chemistry** in the Eastern sites chapter (Expedition 357 Scientists, 2017a), methane concentrations ranged from below the detection limit to 48 µM, and hydrogen concentrations varied from trace levels to 323 µM (see Table **T12** in the Eastern sites chapter [Expedition 357 Scientists, 2017a]). Hot spots of hydrogen were observed over Sites M0068–M0072, and hot spots of methane were observed over Sites M0070–M0072 (see Figure **F26** in the Eastern sites chapter [Expedition 357 Scientists, 2017a]).

Microbiology

Samples collected

Following the procedure described in detail in **Microbiology** in the Expedition 357 methods chapter (Expedition 357 Scientists, 2017b), whole-round core (WRC) samples were transferred to the cold room after they were photographed.

At Site M0070, five WRC samples were collected for microbiological studies: two from Hole M0070A (2R-1 and 3R-1), one from Hole M0070B (1R-1), and two from Hole M0070C (1R-1 and 3R-1) (Table **T3**; see MBIOWRC in **Supplementary material**). These samples were divided into five unflamed frozen samples, four flamed frozen samples, three enrichment samples, four exterior PFC samples, three interior PFC samples, four exterior cell count samples, three interior cell count samples, and four single-cell analysis samples. Additional exterior cell count samples were taken adjacent to the microbiology whole-round samples at the top of Sections 357-M0070C-1R-1 and 3R-1.

At Site M0074, one 0.86 m carbonate sediment core (Section 1R-1) was recovered, from which microbiological samples were collected immediately by inserting 10 mL cut-off sterile syringes at 0.1–0.2 and 0.5–0.6 mbsf. The sediment is mainly composed of calcareous sand. From each depth interval, we took three samples for shipboard enrichment culturing, one for exterior PFC samples, one for CH_4/H_2 gas analyses, one for exterior cell count samples, and one for single-cell analysis (Table **T3**).

Samples to be sent to Kochi Core Center (Japan) were immediately frozen at –80°C and then shipped under temperature-controlled conditions with constant temperature logging. There, WRC exteriors will be cut away with a band saw system equipped in a clean booth and used for perfluoromethylcyclohexane (PFC) tracer check (exterior), concentration and isotopic composition of total inorganic carbon (TIC)/total organic carbon (TOC), vein analysis, in situ organic carbon and Fe mineral analysis, and trapped-gas analysis. The interior portion of the frozen samples will be subjected to shore-based nucleic acid analyses and interior PFC, organic, and lipid analyses.

Liner fluid from the core barrels was collected from many cores from each site and was split for PFC, cell count, and organic acid analyses (Table **T4**).

Table T3. Whole-round cores collected for microbiological analysis, Sites M0070 and M0074. **Download table in .csv format.**

Table T4. Core liner fluid samples for microbiological analyses, Sites M0070 and M0074. **Download table in .csv format.**

Table T5. Microbial cell abundance counted on flame-sterilized interior piece of rock samples, Site M0070. **Download table in .csv format.**

Contamination assessment with PFC tracer

Samples of liner fluid, sensor package Niskin bottles, and exterior and interior pieces of WRCs were collected to assess contamination by quantifying the concentration of PFC tracer added during drilling operations (see **Microbiology** in the Expedition 357 methods chapter [Expedition 357 Scientists, 2017b]). Laboratory atmosphere blanks are also reported in Table **T15** in the Eastern sites chapter (Expedition 357 Scientists, 2017a) to define lower detection limits; these values varied throughout the expedition because of buildup of volatilized tracer in the shipboard laboratory. PFC concentrations for samples are reported in picograms PFC per cubic centimeter of sample, and laboratory blanks are reported as picograms PFC per milliliter air.

PFC delivery during drilling operations was successful in all Site M0070 holes based on generally high concentrations (10^1–10^4 pg PFC/mL sample) of tracer in the sensor package and liner fluid samples (see Table **T15** in the Eastern sites chapter [Expedition 357 Scientists, 2017a]). Exterior WRC samples also generally had high PFC concentrations. Some interior WRC samples after flame sterilization of the exterior had lower tracer concentrations, but other interior samples were roughly equivalent in concentration, which likely reflects the porous nature of the basalt breccia that dominated these sample types. PFC delivery during drilling operations at Site M0074 was weak, with low PFC concentrations detected.

Cell abundance determination

Cell abundance was determined by direct counting with an epifluorescence microscope (see **Microbiology** in the Expedition 357 methods chapter [Expedition 357 Scientists, 2017b]). For shipboard analysis of select rock samples, flame-sterilized interior cell count samples were crushed into millimeter-sized grains, and then 3 cm^3 was taken for fixation. Minimum quantification limits of the cell counting methods were determined by analysis of procedural negative controls and determined to be 48 cells/cm^3.

Cell abundance was very low on the one sample examined from Site M0070 (Table **T5**). Cell density was 3.6×10^2 cells/cm^3 at 0.3 mbsf. No shipboard cell counts were made on sediment samples from Hole M0074A; these will be measured in a shore-based laboratory.

Enrichment and incubation experiments

The growth and activity of microbial communities was studied in rock samples obtained during the expedition using a variety of culture-based approaches. Flame-sterilized pieces of rock material were ground to fine particles under anoxic conditions and distributed into the various incubation vessels (Table **T3**; see **Microbiology** in the Expedition 357 methods chapter [Expedition 357 Scientists, 2017b]).

Samples were used in the following ways:

- To study microbe-rock interactions (Sections 357-M0070B-1R-1 and 357-M0070C-1R-1);

Table T6. Water samples collected from sensor package Niskin bottles for microbiological analysis, Site M0070. **Download table in .csv format.**

Table T7. Water samples collected from CTD rosette Niskin bottles for microbiological analysis, Sites M0070 and M0074. **Download table in .csv format.**

- To initiate experiments to study the growth of anaerobic microorganisms at elevated hydrostatic pressures (Section 357-M0070C-3R-1);
- To evaluate the presence of hydrogenotrophic and/or methanogenic microorganisms, as well as heterotrophic microorganisms, under alkaline, anoxic conditions (Section 357-M0070C-3R-1);
- To study the growth of microorganisms under sulfate-reducing conditions (Section 357-M0074B-1R-1);
- To study the growth of microorganisms at elevated hydrostatic pressures (Section 357-M0074B-1R-1); and
- To study the assimilation of stable isotope–labeled carbon and nitrogen compounds (Section 357-M0074B-1R-1).

Water samples for microbiological analysis

Water from sensor package Niskin bottles and CTD rosette Niskin bottles was subsampled for measurements of PFC, cell counts, and DNA from Sites M0070 and M0074 (Tables **T6**, **T7**) and for many chemical measurements (see **Water sampling and sensor package data** in the Expedition 357 methods chapter [Expedition 357 Scientists, 2017b]).

Sensor package data

Mapping drill data onto the sensor plots for all sites was done graphically, and for records of approximately 1000 min, the potential errors are on the order of ±5 min.

Hole M0070A

In Hole M0070A, a significant CH_4 peak (55 nM) at 1264 mm in Core 1R corresponded to a drop in oxidation-reduction potential (ORP) and, as at other sites, was reflective of more reducing fluid reaching the sensors (Figure **F7**; Table **T8**). A second, smaller CH_4 peak (35 nM) at 1781 mm coincided with the changeover between Cores 1R and 2R and was likely a result of the lack of flushing water diluting the signals. As mentioned in **Operations**, bubbles were observed emanating from the borehole during drilling at Hole M0070A, and these were followed by a noticeable deviation in the methane signal. As at the western sites, CH_4 background values were high, ranging from 30 nM at the start of drilling to 15 nM at the end. The pH values ranged from about 7.90 at the beginning of drilling to about 7.98 at the end.

Hole M0070B

Hole M0070B was shallow (1300 mm) with only 38 mm recovery. There were no significant sensor signals, and therefore the data are not shown.

Hole M0070C

The sensor data from drilling Hole M0070C extended over 1300 min, which is split into two data plots (Figure **F8**; Table **T9**). Two small CH_4 peaks at 2012 h (22.7 nM) and 2036 h (22.5 nM) occurred prior to the start of drilling, likely a result of the drill disturbing the sediments upon landing (Figure **F8A**). A small CH_4 peak (23.7 nM) was seen just after drilling started Core 1R at 390 mm. A second CH_4 peak (24.2 nM) was seen at the end of Core 1R at 1146 mm. This peak was coincident with lifting the drill string out of the hole to replace the BHA. Neither of these two CH_4 peaks coincided with a significant drop in ORP. A few minutes after the CH_4 peak (22.5 nM) at 0017 h (2421 mm), bubbles were seen emanating from the region of the drill base. This occurred while Core 2R was being drilled and coincided with the minimum of a large negative anomaly in ORP that began at 2310 h and ended at 0229 h. All three of these CH_4 peaks coincided with significant shifts in pH. There was also a significant CH_4 peak associated with the end of drilling Core 3R at 0328 h (23 nM). Another CH_4 peak occurred at 0457 h (24.3 nM) on the attempt to drill Core 4R just after drilling stopped and the drill string was raised slightly. Background CH_4 values remained high throughout this drilling period, starting at 22.2 nM and ending at 18.4 nM.

The MeBo remained on the bottom for an additional several hours while attempting to deepen the hole (Figure **F8B**). During this period, several CH_4 and ORP peaks were observed. A small CH_4 peak occurred at 0817 h with no ongoing drilling operations to produce it. It seems likely that this peak was caused by the many gas bubbles seen around the drill at this time. A large CH_4 excursion started at 0845 h, with three separate peaks (34 nM at 0851 h, 26 nM at 0855 h, and 36 nM at 0859 h). These peaks are best seen in an expanded plot (Figure **F8C**). The drill video shows that the beginning of each of these peaks occurred when the drill bit was pulled out of the hole, with the peak being reached just as the bit reentered the hole. The signal reached background levels after the bit was pushed below what seemed to be a level of high gas concentration at a relatively shallow depth in the hole. The 0851 h event is shown in Figure **F8D**, where material can be seen pouring out of the drill bit and onto the sensor intake tube. The drilling data file ends at 1053 h (Table **T9**), so bit depth is unknown beyond this time, but drill video can be used to interpret sensor data late in the deployment. The entire broad CH_4 peak starting at 1110 h and ending at 1246 h took place with the hole open and nothing happening with the drill to produce the signal (Figure **F8B**). Again, voluminous gas bubbles were seen during this period and throughout the time the drill remained on site. These bubbles could have been the source of the unusually high CH_4 values. The two small CH_4 peaks seen at 1301 and 1333 h and the ORP minimum that started at 1250 h and reached a minimum at 1320 h also occurred under open-hole conditions. The large (32.5 nM) CH_4 peak that started at 1437 h began at the same time as the bit was lowered into the hole and drilling started. At 1444 h, just before the CH_4 peak at 1447 h, a burst of material was seen coming out of the drill hole. Drilling was stopped at 1456 h, and the drill string was immediately pulled out of the hole. The CH_4 peak did not reach background levels until 1537 h, at which point the drill had been lifted 234 m off the seafloor.

Hole M0074A

Hole M0074A is a shallow, one-core hole that obtained only carbonate sediments. The site was too deep (1549 m) to utilize the pH/ORP electrode, and the dissolved oxygen probe did not function properly. Background CH_4 values were again high, ranging from 25.8 to 24.2 nM. There was a small CH_4 peak (28.2 nM) (Figure **F9**; Table **T10**), but it appeared to be a result of the drill landing on the seafloor because it peaked at about the same time as the drilling of Core 1R started.

Figure F7. Sensor data, Hole M0070A. Elapsed time = time since the start of the sensor package data file. Penetration depth is from drill logs.

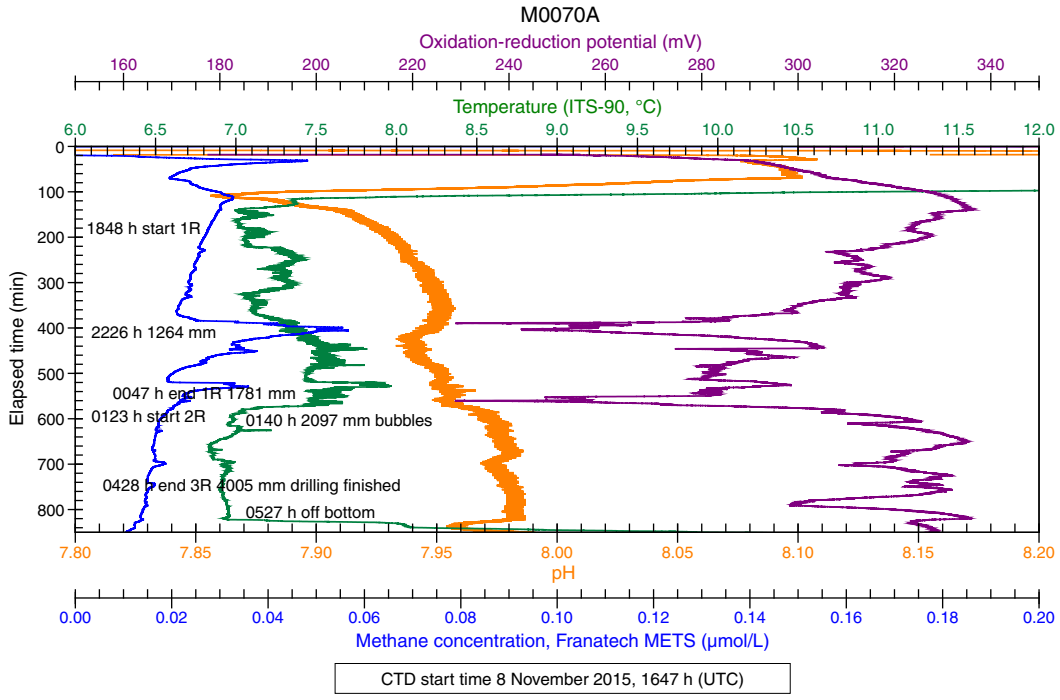

Table T8. Sensor signal time log, Hole M0070A. **Download table in .csv format.**

Figure F8. Sensor data, Hole M0070C. Three cores were recovered from this hole. No coring occurred after 0325 h because the MeBo remained on the seafloor with operational problems. A, B. Elapsed time = time since the start of the sensor package data file. Penetration depth is from drill logs. (Continued on next two pages.).

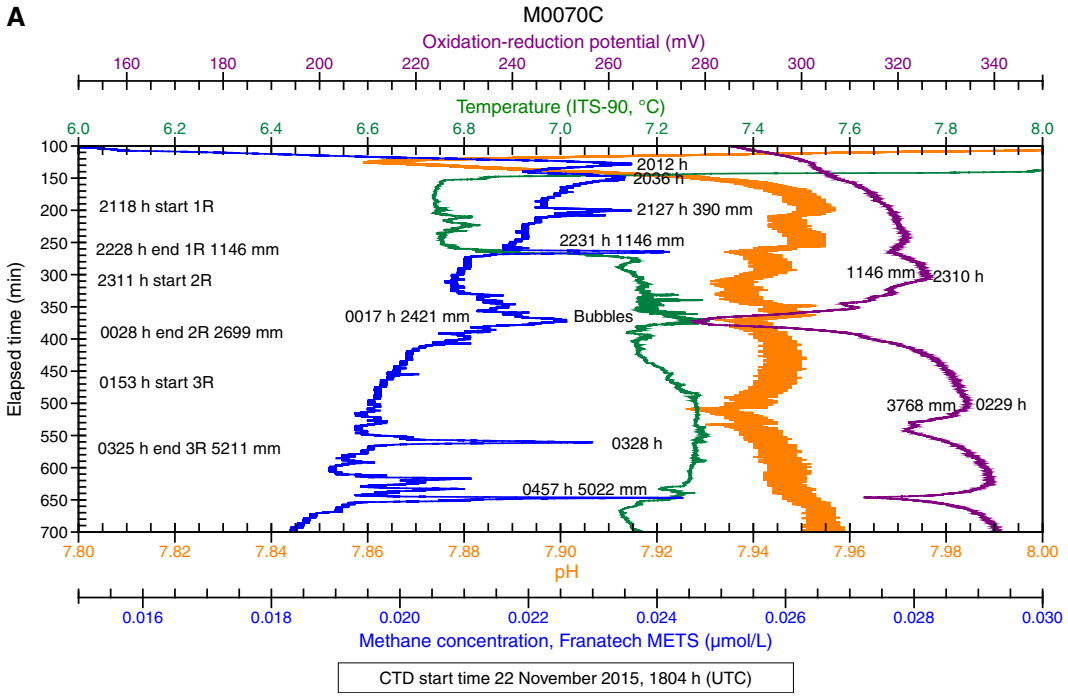

Figure F8 (continued). C. 1 h segment of data in B. (Continued on next page.)

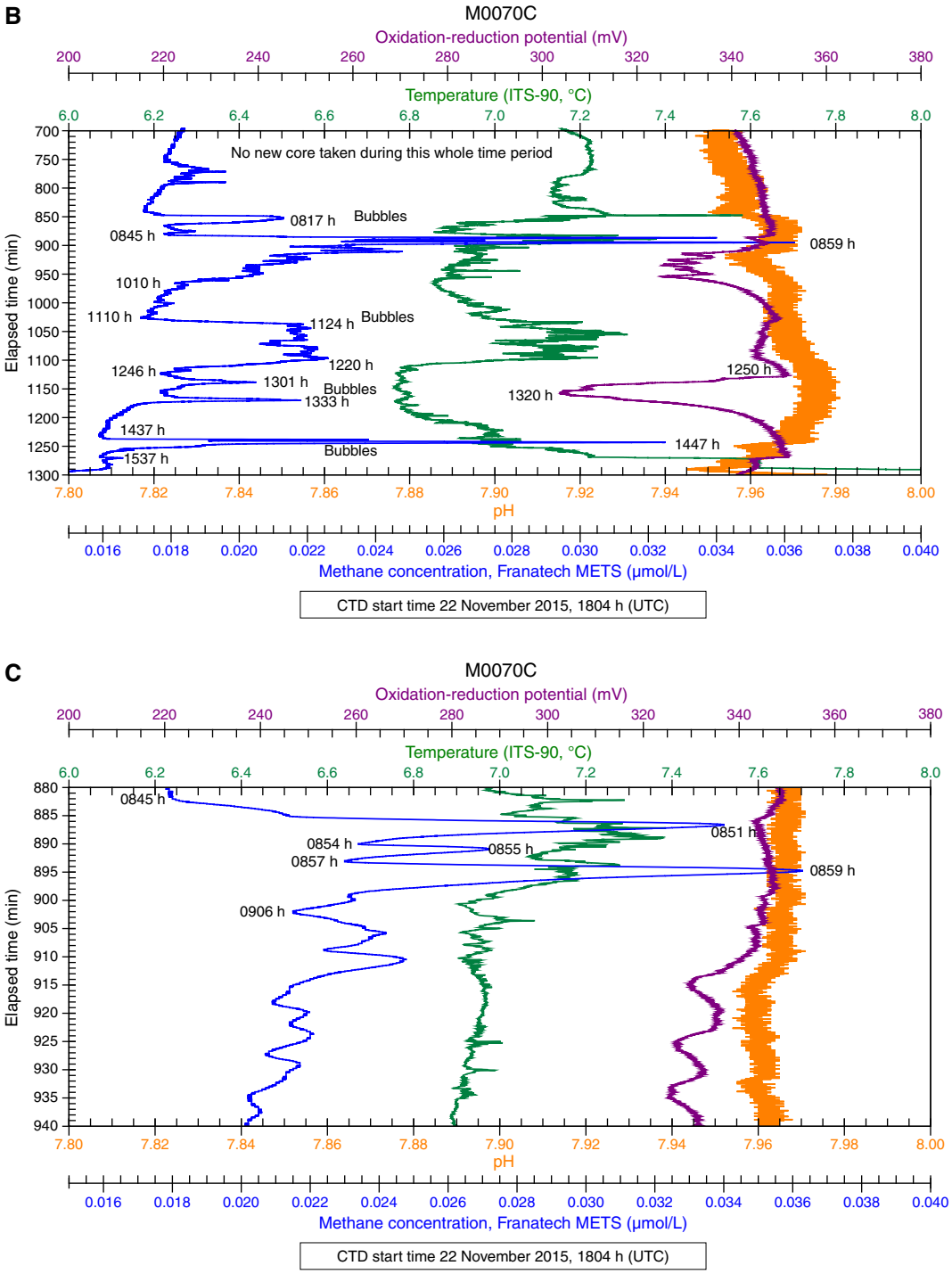

Figure F8 (continued). D. Frame grab from MeBo video showing material flowing out of core barrel at 0851 h on 23 November 2015.

Table T9. Sensor signal time log, Hole M0070C. **Download table in .csv format.**

Figure F9. Sensor data, Hole M0074A. Elapsed time = time since the start of the sensor package data file. Penetration depth is from drill logs.

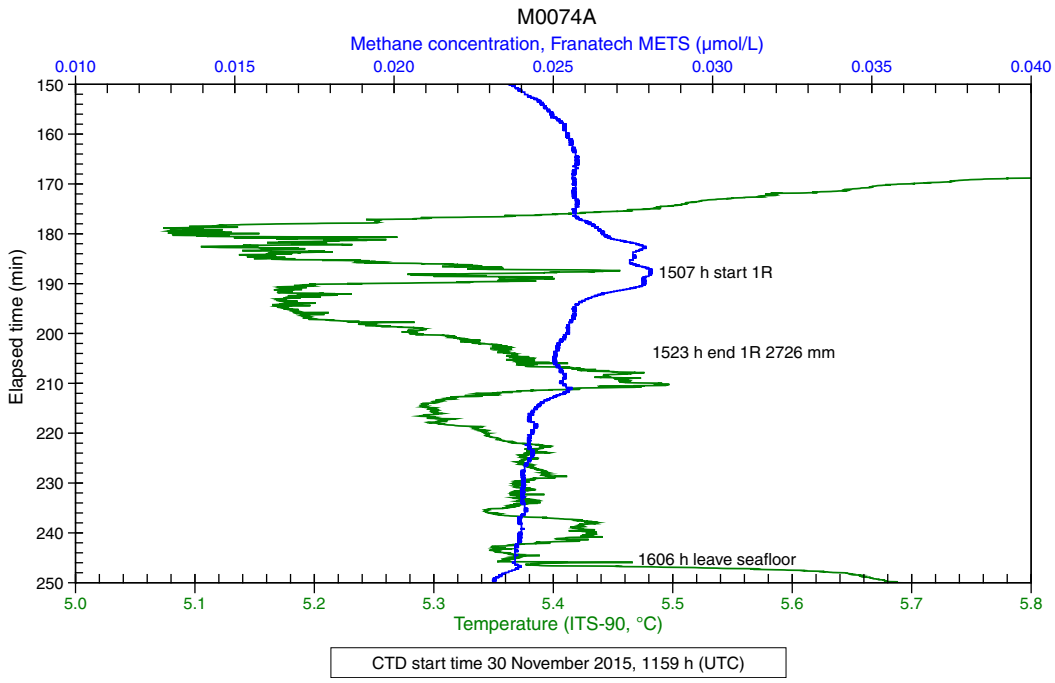

Table T10. Sensor signal time log, Hole M0074A. **Download table in .csv format.**

Table T11. Grain density, porosity, and *P*-wave velocity for discrete sample, Site M0070. **Download table in .csv format.**

Physical properties

Site M0070

A total of 4.68 m of core was recovered from the three holes at Site M0070: ≈52% in Hole M0070A (4.00 mbsf), ≈29% in Hole M0070B (1.30 mbsf), and ≈42% in Hole M0070C (5.21 mbsf).

Density and porosity

Gamma density (GD) at Site M0070 has a mean of 2.21 g/cm^3 but scatters significantly between 1.28 and 2.75 g/cm^3. Because these cores are composed almost exclusively of basalt breccia with a calcareous matrix, these variations are strongly influenced by the different densities of clasts and matrix and the variability in the relative proportion of the different components with depth.

Moisture and density (MAD) measurements were conducted on metadolerite Sample 357-M0070C-1R-1, 38.5–40.5 cm (0.39 mbsf), and returned a grain density of 2.96 g/cm^3 and a porosity of 4.1%.

P-wave velocity

One discrete metadolerite sample (357-M0070C-1R-1, 38.5–40.5 cm) (Table **T11**) was obtained at Site M0070. *P*-wave velocity along the *x*-direction (horizontal) is 5.19 km/s. The second horizontal direction, the *y*-direction, has a lower *P*-wave velocity (4.75 km/s). *P*-wave velocity measured along the *z*-direction (vertical) is 4.75 km/s. The mean *P*-wave velocity of this sample is 4.90 km/s.

Electrical resistivity

Electrical resistivity at Site M0070 is low to moderate with a mean value of 8.8 Ωm and a range of 1.2 to 19.9 Ωm. Holes M0070A and M0070C have similar low values in their uppermost cores, below which resistivity values are more elevated. Electrical resistivity increases from the thin layer of carbonate sand at the top of Hole M0070A to the underlying basalt breccia and varies significantly within the breccia. In Hole M0070A, local resistivity maxima occur at 0.36, 1.92, 2.24, 3.04, 3.28, and 3.42 mbsf. A net increase in resistivity with depth is punctuated by maxima at 0.06, 0.30, 0.48, 1.21, 1.49, 1.61, 2.88, and 3.26 mbsf. Hole M0070B has the lowest resistivity values (<5 Ωm).

Magnetic susceptibility

Magnetic susceptibility at Site M0070 has a mean value of 195 × 10^{-5} SI and ranges from 34 × 10^{-5} to 967 × 10^{-5} SI. Minima occur at the same depths as electrical resistivity maxima. Similarly, the overall increase in resistivity with depth in Hole M0070C is mirrored by a decrease in magnetic susceptibility.

Natural gamma radiation

Scatter in the natural gamma radiation (NGR) data sets (Figures **F10**, **F11**, **F12**) is comparable to that of gamma density. NGR is very low across Site M0070. In Hole M0070A, the uppermost core has elevated NGR intensity compared to the deeper cores, which exhib-

Figure F10. Physical properties, Hole M0070A. Color reflectance: black = L*, red = a*, blue = b*.

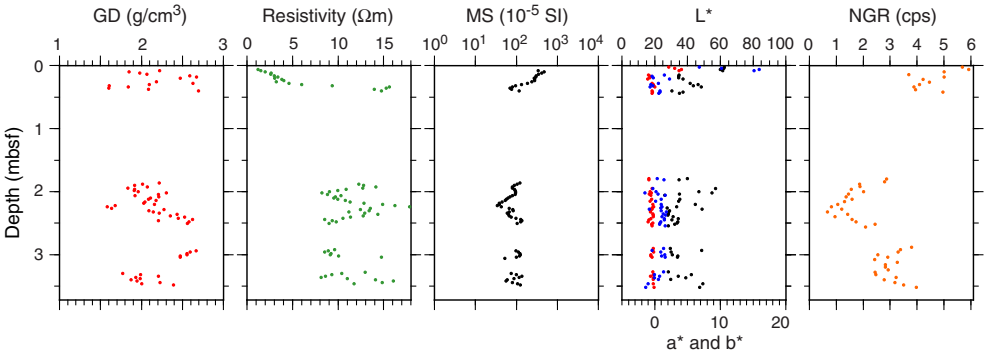

Figure F11. Physical properties, Hole M0070B. Color reflectance: black = L*, red = a*, blue = b*.

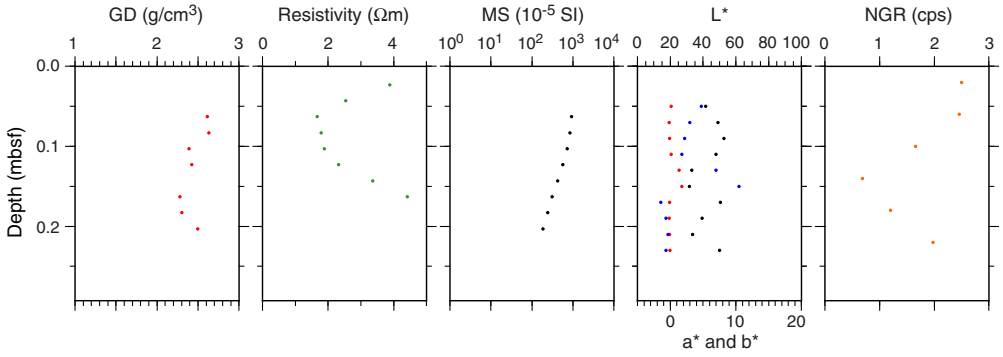

Figure F12. Physical properties, Hole M0070C. MAD: red circle = bulk density, green circle = dry density, blue circle = grain density. *P*-wave: open circle = *x*-direction, blue dot = *y*-direction. Color reflectance: black = L*, red = a*, blue = b*.

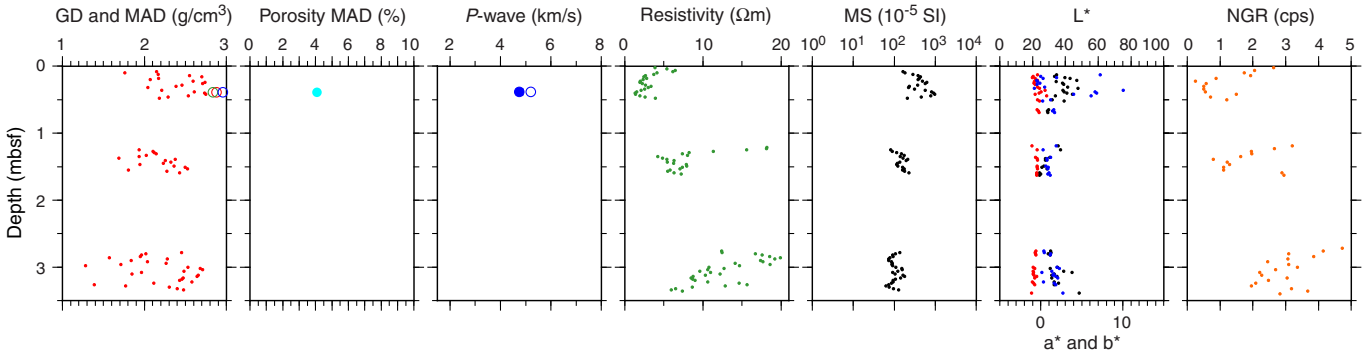

its an overall increase with depth. This net increase with depth is also present in Hole M0070C.

Color reflectance

The lightness (L*) of Hole M0070A cores ranges from 26.18% to 62.38% with a mean value of 38.54%. a* and b* have mean values of −0.18 (range = −1.06 to 4.08) and 1.50 (range = −1.51 to 15.90), respectively. The uppermost section (Section 1R-1) returns significantly greater scatter in the color reflectance data than deeper cores. The deeper cores have relatively constant a* and b* values close to zero (Figure **F10**; Table **T12**).

In Hole M0070B, a whole-round sample of 13 cm was taken for microbiology, so there are only a limited number of color reflectance measurement points. L* ranges from 31.62% to 52.78% with a mean of 42.99%. a* and b* have mean values of 0.27 (range = −0.18 to 1.79) and 2.61 (range = −1.42 to 10.50), respectively (Table **T12**).

The L* of Hole M0070C cores varies between 24.12% and 48.49% with a mean of 34.56%. Reflectance parameter a* has a very small range (−1.12 to 0.73) with a mean of −0.57. Reflectance parameter b* varies more significantly from −0.79 to 10.05 with a mean of 1.67. The large scatter in b* is only observed within the shallowest core; for the deeper cores, the standard deviation of the measurements is rather small. This small standard deviation is not, however, an indication of homogeneous core but instead a consequence of sampling bias. Measurements were taken on clasts not affected by fractures or cracks and on 8 mm spots that do not exhibit high color contrast (see **Physical properties** in the Expedition 357 methods chapter [Expedition 357 Scientists, 2017b]).

Site M0074

One hole was drilled at Site M0074. Approximately 31% of the drilled depth (2.68 mbsf) was recovered with 0.86 m of core in this northernmost hole drilled during Expedition 357 (Hole M0074A).

Density and porosity

Site M0074 sediments have a mean gamma density of 1.65 g/cm^3 with a narrow range of 1.57–1.72 g/cm^3. There is no net change in gamma density with depth, and the profile is largely featureless.

Because the sediment core from Site M0074 was highly disturbed while being transferred from a metal split liner to a plastic liner, this core was not subsampled for MAD analyses.

Table T12. Physical properties, Sites M0070 and M0074. **Download table in .csv format.**

P-wave velocity

No discrete samples were taken for physical properties analyses at Site M0074. *P*-wave velocity measurements are therefore absent from the data set.

Electrical resistivity

Electrical resistivity is extremely low with a mean of 0.8 Ωm, a minimum of 0.6 Ωm, and a maximum of 1.1 Ωm. A subtle net decrease in resistivity with depth was observed (Figure **F13**).

Magnetic susceptibility

Similar to electrical resistivity, magnetic susceptibility is very low with a mean of 9 × 10^{-5} SI and a range of 6 × 10^{-5} to 15 × 10^{-5} SI. The interval between 0.3 and 0.5 mbsf is slightly elevated (>10 × 10^{-5} SI) in magnetic susceptibility compared to the material above and below.

Natural gamma radiation

As is characteristic for the lithologies sampled across Atlantis Massif, NGR intensities are extremely low. There are no systematic changes in the profile with depth (Figure **F13**).

Color reflectance

L* (lightness) varies from 61.95% to 75.58% with a mean of 65.33%, indicating a dominance of light material in this hole. Reflectance parameter a* varies from 3.08 to 6.37, and b* varies from 18.29 to 24.21. The mean values of a* and b* are 4.99 and 215, respectively, representing yellow and orange colors. All three CIELab color space dimensions (L*, a*, and b*) have very low standard deviations (Figure **F13**; Table **T12**), indicating homogeneity, which is consistent with the sediments recovered.

Summary

Physical properties from the ≈5.5 m of core recovered across the four holes drilled in the northern area were acquired during the expedition, including MAD and *P*-wave velocity analyses on one discrete sample. There are significant differences between the two sites sampled in the Northern area because Site M0074 was drilled through unconsolidated calcareous sediment and Site M0070 sampled lithified material. It is therefore not appropriate to directly compare the sites.

Site M0070 is characterized by moderate intensities of magnetic susceptibility and some intervals of elevated electrical resistivity. These two parameters are systematically anticorrelated. The basal-

Figure F13. Physical properties, Hole M0074A. Color reflectance: black = L*, red = a*, blue = b*.

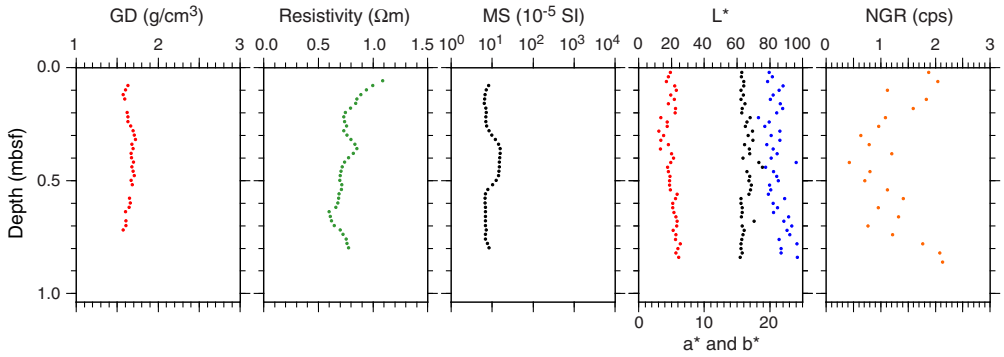

tic breccia of the uppermost 0.5 m in each of the holes has enhanced lightness and higher b* values compared to material deeper in the holes (M0070A and M0070C; Hole M0070B only sampled the breccia).

The northernmost of all of the Expedition 357 sites, Site M0074, is characterized by very low density, magnetic susceptibility, and resistivity. L* is very high and b* is also elevated, testament to the pale yellowish calcareous sediments recovered.

References

Blackman, D.K., Karson, J.A., Kelley, D.S., Cann, J.R., Früh-Green, G.L., Gee, J.S., Hurst, S.D., John, B.E., Morgan, J., Nooner, S.L., Ross, D.K., Schroeder, T.J., and Williams, E.A., 2002. Geology of the Atlantis Massif (Mid-Atlantic Ridge, 30°N): implications for the evolution of an ultramafic oceanic core complex. *Marine Geophysical Research,* 23(5–6):443–469. **http://dx.doi.org/10.1023/B:MARI.0000018232.14085.75**

Früh-Green, G.L., Orcutt, B.N., Green, S.L., Cotterill, C., Morgan, S., Akizawa, N., Bayrakci, G., Behrmann, J.-H., Boschi, C., Brazelton, W.J., Cannat, M., Dunkel, K.G., Escartin, J., Harris, M., Herrero-Bervera, E., Hesse, K., John, B.E., Lang, S.Q., Lilley, M.D., Liu, H.-Q., Mayhew, L.E., McCaig, A.M., Menez, B., Morono, Y., Quéméneur, M., Rouméjon, S., Sandaruwan Ratnayake, A., Schrenk, M.O., Schwarzenbach, E.M., Twing, K.I., Weis, D., Whattam, S.A., Williams, M., and Zhao, R., 2017a. Eastern sites. *In* Früh-Green, G.L., Orcutt, B.N., Green, S.L., Cotterill, C., and the Expedition 357 Scientists, *Atlantis Massif Serpentinization and Life.* Proceedings of the International Ocean Discovery Program, 357: College Station, TX (International Ocean Discovery Program). **http://dx.doi.org/10.14379/iodp.proc.357.103.2017**

Früh-Green, G.L., Orcutt, B.N., Green, S.L., Cotterill, C., Morgan, S., Akizawa, N., Bayrakci, G., Behrmann, J.-H., Boschi, C., Brazelton, W.J., Cannat, M., Dunkel, K.G., Escartin, J., Harris, M., Herrero-Bervera, E., Hesse, K., John, B.E., Lang, S.Q., Lilley, M.D., Liu, H.-Q., Mayhew, L.E., McCaig, A.M., Menez, B., Morono, Y., Quéméneur, M., Rouméjon, S., Sandaruwan Ratnayake, A., Schrenk, M.O., Schwarzenbach, E.M., Twing, K.I., Weis, D., Whattam, S.A., Williams, M., and Zhao, R., 2017b. Expedition 357 methods. *In* Früh-Green, G.L., Orcutt, B.N., Green, S.L., Cotterill, C., and the Expedition 357 Scientists, *Atlantis Massif Serpentinization and Life.* Proceedings of the International Ocean Discovery Program, 357: College Station, TX (International Ocean Discovery Program). **http://dx.doi.org/10.14379/iodp.proc.357.102.2017**

Früh-Green, G.L., Orcutt, B.N., Green, S.L., Cotterill, C., Morgan, S., Akizawa, N., Bayrakci, G., Behrmann, J.-H., Boschi, C., Brazelton, W.J., Cannat, M., Dunkel, K.G., Escartin, J., Harris, M., Herrero-Bervera, E., Hesse, K., John, B.E., Lang, S.Q., Lilley, M.D., Liu, H.-Q., Mayhew, L.E., McCaig, A.M., Menez, B., Morono, Y., Quéméneur, M., Rouméjon, S., Sandaruwan Ratnayake, A., Schrenk, M.O., Schwarzenbach, E.M., Twing, K.I., Weis, D., Whattam, S.A., Williams, M., and Zhao, R., 2017c. Expedition 357 summary. *In* Früh-Green, G.L., Orcutt, B.N., Green, S.L., Cotterill, C., and the Expedition 357 Scientists, *Atlantis Massif Serpentinization and Life.* Proceedings of the International Ocean Discovery Program, 357: College Station, TX (International Ocean Discovery Program). **http://dx.doi.org/10.14379/iodp.proc.357.101.2017**